

Fault Diagnosis of Induction Motor Based on a Novel Intelligent Framework and Transient Current Signals

Van Tung Tran*, Robert Cattley, Andrew Ball, Bo Liang, Simon Iwnicki

School of Computing and Engineering, University of Huddersfield, Queensgate, Huddersfield HD1 3DH, UK.
V.T.Tran@hud.ac.uk

This paper deals with fault diagnosis of induction motor containing common faults by using a novel intelligent framework and transient stator current signals. This framework consists of a Fourier-Bessel (FB) expansion for analyzing the transient signals, a generalized discriminant analysis (GDA) for feature reduction, and a relevance vector machine (RVM) for fault classification. The start-up transient current signals are acquired from different motor operating conditions and decomposed into single components using FB expansion. Subsequently, a number of statistical features in the time domain and the frequency domain are computed for each component to represent the motor conditions. The high dimensionality of the feature set is reduced by implementing GDA. Finally, the diagnosis performance is carried out by RVM, which is an intelligent method in pattern recognition area. The framework has been applied for traction motor faults including bowed rotor, broken rotor bar, eccentricity, faulty bearing, mass unbalance, and phase unbalance in general applications. The results show that the proposed diagnosis framework is capable of improving the classification accuracy significantly in comparison other methods.

1. Introduction

Induction motors are one of the most widely used electrical machines in industry due to their ruggedness and versatility. However, they are susceptible to many types of fault sourced from mechanical and electrical stresses which permanently exist in motor's operation. According to motor reliability study (Bonnett, 1992), the faults in induction motor are typically related to bearings, stator, rotor, and the remainder that is a consequence of a great variety of other faults. These faults are often sources of increasing the maintenance costs, disturbances in production activity, and the main reason for stoppage of operation. Therefore, reliable diagnostic frameworks are of necessity to enable effective maintenance and operational costs.

In order to detect and identify these faults, motor current signature analysis (MCSA) is a widely and early used scheme. Many studies have been developed based on MCSA under steady state operating conditions. For instance, Schoen (Schoen et al., 1995) and used MCSA for detecting the rolling-element bearing damage in induction machines. Thomson (Thomson and Fenger, 2001) focused on the industrial application of MCSA to fault diagnosis in three-phase induction motor drives. However, MCSA depends not only on the accuracy of measurements, but also on the ability to differentiate between normal and faulty conditions (Henry et al., 2002). Furthermore, the techniques using steady state conditions are effectively used only when the machines are almost fully loaded and running at a constant speed. Conversely, they result in less accuracy when applied to machines that are lightly loaded or operated predominantly under transient conditions (Douglas and Pillay, 2005).

Transient signals have been attracted attention in recent times due to the fact that the machine is subjected to stresses above normal condition during the start-up. These stresses could highlight machine defects that are early in their development and are not easily detected at steady state conditions (Niu et al., 2008). However, transient signals are non-linear, non-stationary, and contains several components. These lead to difficulty in using common methods such as fast Fourier transform (FFT) to analyze the fault symptom in the induction motor. Short-time Fourier transform (STFT) and Hilbert-Huang transform (HHT) are other techniques which were proposed to deal with non-stationary signal. However, STFT also has

limitation which is its fixed time-frequency resolution whilst the limitations of HHT were reported in (Rato et al., 2008). Another outstanding technique is the wavelet transform which has been used for processing the motor transient current signals (Niu et al., 2008; Widodo et al., 2009). However, the wavelet basis function has to be defined a priori and this choice may influence the final results. This is a main drawback of wavelet transform.

Recently, Fourier-Bessel (FB) expansion has been introduced as a suitable technique for non-stationary signal analysis because of that it has unique coefficients for a given signal and the Bessel functions are aperiodic and decay over time (Pachori and Sircar, 2008). FB expansion has been widely used for performing speech-related applications such as speech enhancement, speaker identification, speech recognition and synthesis, etc. In the fault diagnosis area, FB expansion in association with the Wigner-Ville distribution has been used for gear fault study (D'Elia et al., 2012). In this paper, FB expansion is introduced to an intelligent framework as shown in Figure 1 for fault diagnosis of induction motor. This framework involves three stages which are signal decomposition, feature representation and reduction, and classification. In the first stage, the FB expansion is implemented to decompose the transient current signals acquired from induction motor into the FB series. Each single component in the signal is isolated by a non-overlapping cluster of FB coefficients. In the second stage, statistical features in the time domain and the frequency domain are extracted for each component decomposed in the previous stage. The high dimensionality of feature set is reduced by using the generalized discriminant analysis (GDA) (Baudat and Anouar, 2000). In the last stage, relevance vector machine (RVM) (Tipping, 2001), which is a remarkable method of machine learning techniques, is used to identify the faults occurring in the induction motor.

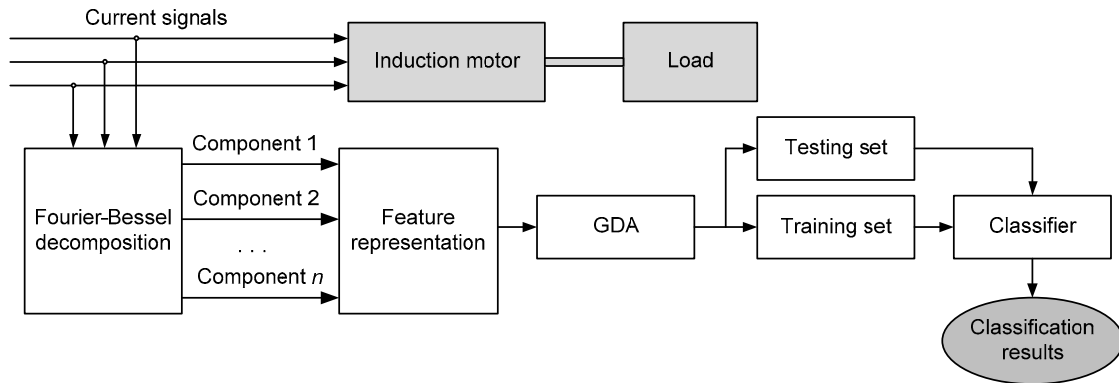


Figure 1: The proposed framework for fault diagnosis

2. Application and discussion

2.1 Experiment and data acquisition

To validate the proposed framework, an experiment was carried out using a test-rig as shown in Figure 2. The load can be changed by adjusting the blade pitch angle or the number of blades. Seven three-phase induction motors of 0.5 kW, 60 Hz, 4-pole were used to generate data. One of these motors is in normal condition (NOR) whilst the others are faulty motors involving bowed rotor (BR), broken rotor bar (BRB), eccentricity (ECC), faulty bearing (outer race) (FBO), mass unbalance (MUN), and phase unbalance (PUN). The conditions of these motors are described in Table 1. For acquiring data from test rig, three AC current probes were used to measure the stator current of the three-phase power supply. The data sample was 16,384 at a sampling rate of 12,800 Hz under a fixed load condition. For each condition, 20 samples were taken.

2.2 FB expansion based signal decomposition

Due to the fact that the data obtained from different motor conditions are non-stationary and contain the line frequency, the current signals of different conditions become similar, which leads to increasing difficulty of classification. To solve this issue, smoothing and subtracting techniques are normally used to reduce/remove the line frequency. However, smoothing the signal could also eliminate useful information which reduces classification accuracy. In this paper, FB decomposition is directly applied to transient current signals to separate them into single component signals so that elimination of useful information is avoided.



Figure 2: Test rig for experiment

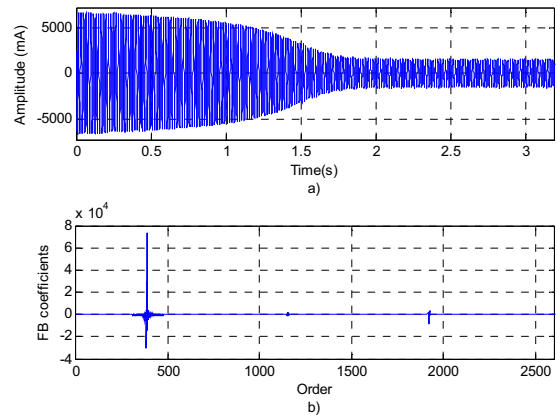


Figure 3: a) Transient current signal of the bowed rotor in phase A, b) FB coefficients

Table 1: The description of motor conditions

Fault Conditions	Fault description	Notes
Bowed rotor	Maximum bowed shaft deflection: 0.075 mm	Air-gap: 0.25 mm
Broken rotor bar	Number of broken bars: 12	Total number of 34 bars
Eccentricity	Parallel and angular misalignments	Adjusting the bearing pedestal
Faulty bearing	Spall on the outer raceway	#6203
Mass unbalance	Unbalance mass on the rotor	-
Normal condition	Healthy condition	-
Phase unbalance	Add resistance on one phase	8.4 %

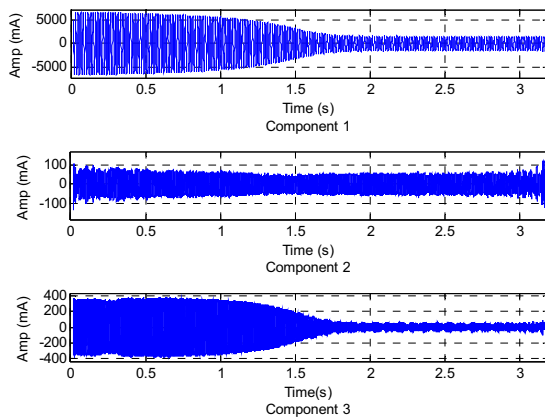


Figure 4: Single components of the bowed rotor signal in phase A

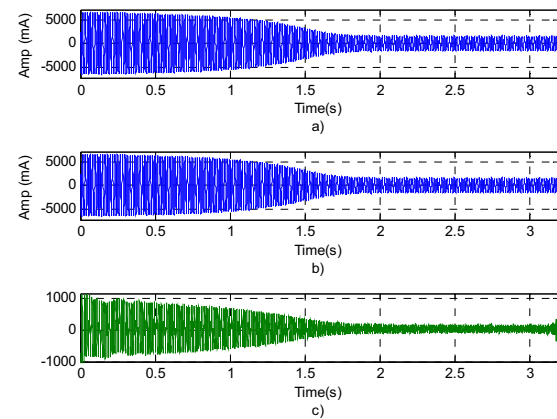


Figure 5: The bowed rotor signal in phase A: a) Original, b) Reconstructed, c) Residual

Figure 3 respectively shows the original transient current signal in phase A of the bowed rotor fault and its FB coefficients. It can be seen in Figure 3(b) that there are three abrupt changes and a distinct cluster of non-overlapping FB coefficients approximately located at the order 380, 1150, and 1900 respectively. These indicate that the original signal is constituted from three single components which can be automatically obtained by choosing proper coefficient bands. Figure 4 shows the single components in a phase of the bowed rotor condition. As observed, the first and the last components are identical in the original signal shape while the second component is significantly different. However, these phenomena are not same in the other conditions where all the components are transient phenomena. The reason is that the single components depend on the values of the FB coefficients. Figure 5 shows a comparison of the

original bowed rotor signal, the reconstructed signal from the three components and the residual in the time domain. As observed from this figure, the original signal could be reconstructed with a high degree of accuracy in shape and amplitude from its single components. However, the residual is still large enough to contain useful information for fault diagnosis; therefore, this residual is used as the last component of the decomposition process. Similarly, the process of identifying the components based on FB coefficients is repeated for the remaining phases (B and C) as well as all the remaining conditions. In total, 1680 ($3 \times 4 \times 140$) components are obtained and used for the next stage.

2.3 Feature representation and reduction

In this study, 21 features are calculated with 10 features in the time domain (mean, RMS, shape factor, skewness, kurtosis, crest factor, entropy error, entropy estimation, and histogram of upper and lower limits) and 3 features in the frequency domain (RMS frequency, frequency center, and root variance frequency). The remaining eight features are auto-regression coefficients. Figure 6 shows the feature structure of each single component where the three-first statistical features (mean, RMS, and shape factor (SF)) are presented. It can be seen in that the features are disorder and overlap with each other which significantly decrease the accuracy of classification result and leads to the misunderstanding of the real machine condition.

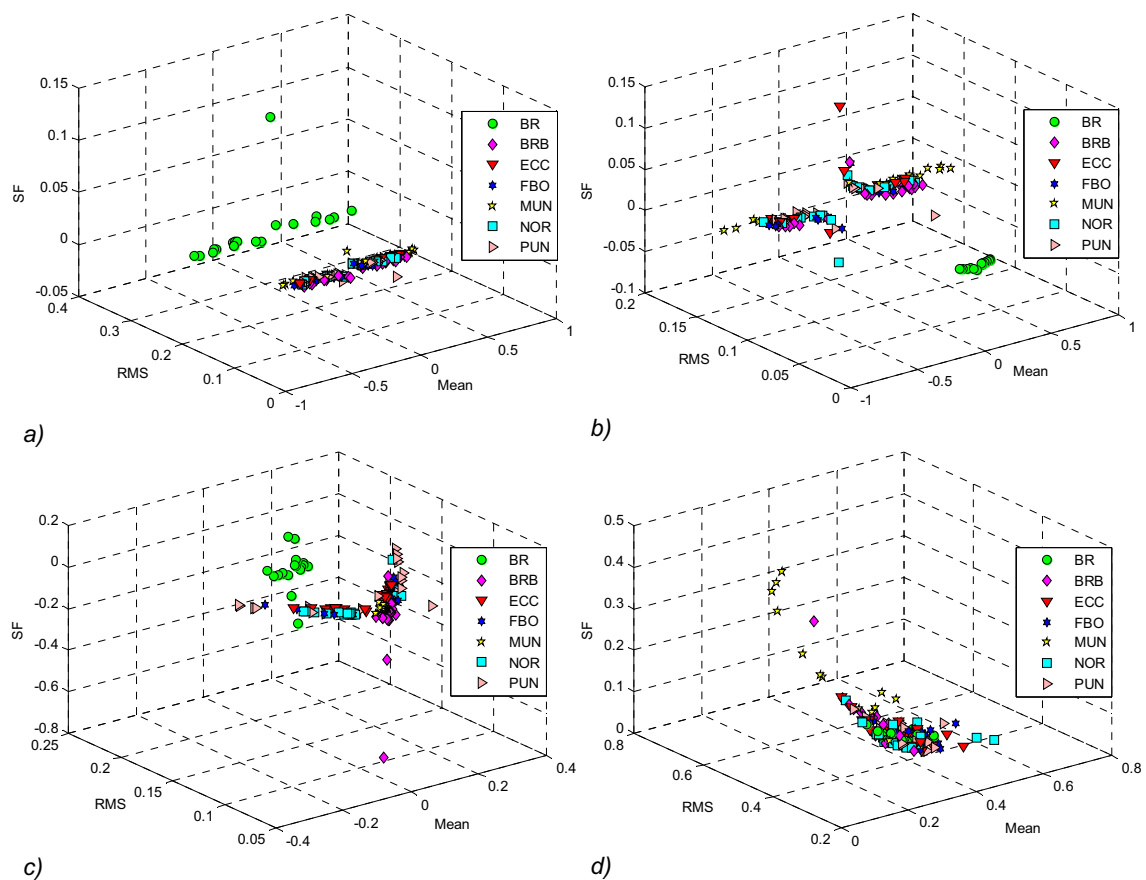


Figure 6: The structure of the three-first features: a) Component 1, b) Component 2, c) Component 3, d) Component 4 (residual)

To reduce the dimensions of the feature set and increase the separation of the feature structure, GDA is subsequently employed on the original features. As a result, sixty-three features in the feature space are reduced to six in the GDA space, which significantly increases computational efficiency. Furthermore, the structures of patterns related to the different conditions are reconstructed as shown in Figure 7. It can be seen that the features of the component 1, component 3, and component 4 of the same condition are located close to each other and are well separated from the other conditions in new space. Thus, the new reduced feature set not only increases the classification performance but also provides an appropriate tool

for a better discrimination of different motor conditions. However, the disorder and overlap still exist in the features of the component 2 which could lead to the inaccuracy in the diagnosis process.

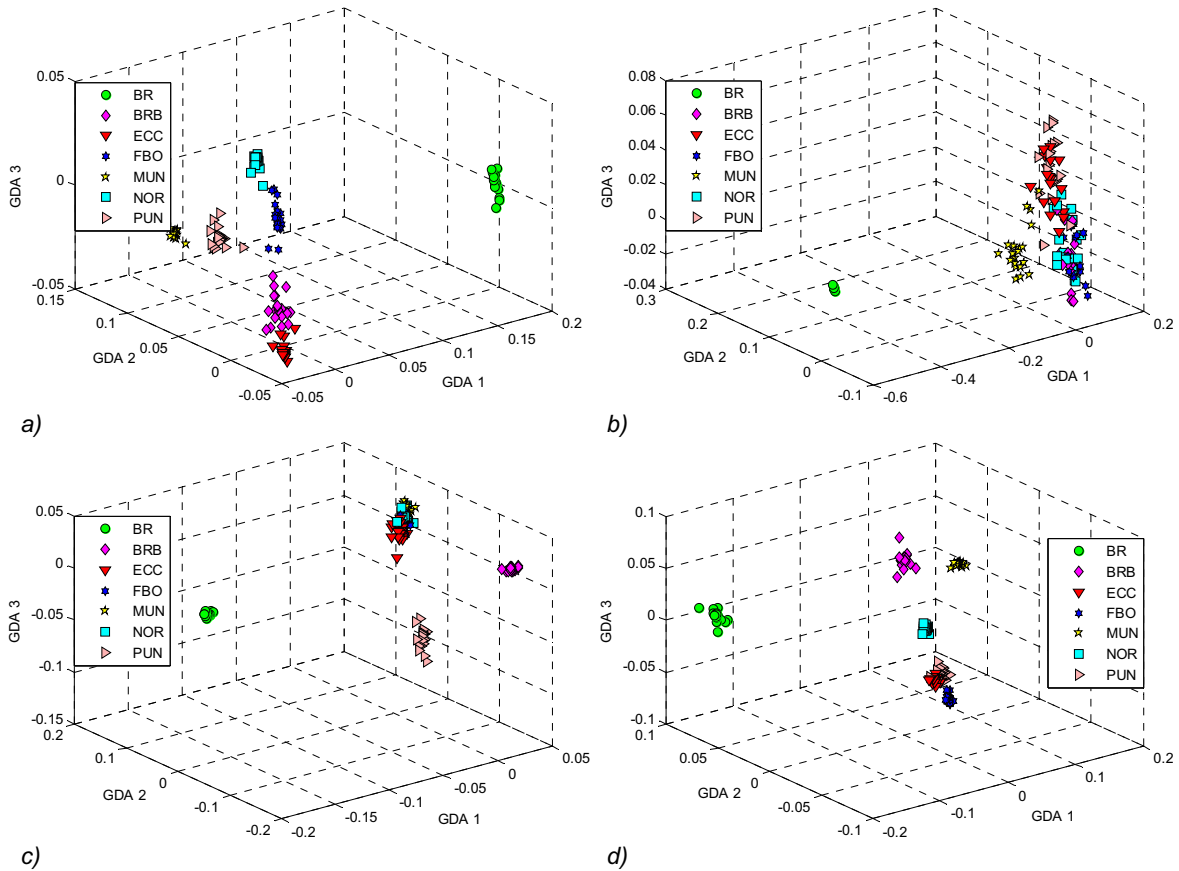


Figure 7: The features in the GDA space: a) Component 1, b) Component 2, c)Component 3, d) Component 4 (residual)

2.4 Classification

In the third stage, the features attained from GDA are inputted to a multiclass RVM classifier. The RBF kernel function is used as the basic function for this classifier and kernel parameter is set to 0.5. Firstly, the feature data set of each component is split into a training set with 10 samples for each condition and a test set with the remaining samples. The classification results of RVM in the training and testing processes are presented in Table 2. As observed, RVM achieves 100 % accuracy in the training process for the component 1, 3, and 4. However, the accuracy for the component 2 is not high as 82.86 %. This is due to the disorder and overlap in the feature structure mentioned in the previous section. In the testing process, the accuracy of the RVM classifiers achieves respectively 97.14 %, 84.29 %, 94.29 %, and 98.57 % for the sequence components. Obviously, the residual gives a better result than the decomposed component. The reason is that the components obtained from the decomposition process have eliminated the similarity caused by the line frequency in the transient signal; hence, the residual can contain useful information characterizing the difference of the machine conditions so that it can attain a higher result.

Table 2: Classification results of RVM

Component	Classification accuracy (%)	
	Training	Testing
1	100	97.14
2	82.86	84.29
3	100	94.29
4	100	98.57

Additionally, in order to emphasize the improvement of the proposed framework where FB expansion is used as a pre-processing tool, support vector machine (SVM) using one-against-all strategy is also implemented as a classifier for the component 4 to compare the performance with the previous studies. The similarity of the kernel parameter is chosen and the regularization in SVM is set as 100. As observed in Table 3, the training accuracy obtained from this study is similar to the previous works and achieves the highest value (100 %). This indicates that the classification model is well trained to diagnose the fault in the test set where the classification accuracy is more important. In the testing process, the framework of this study achieves 98.57 % classification accuracy, which is significantly higher than those of the previous studies. It can conclude that the proposed framework using FB expansion for signal preprocessing has considerably improved the accuracy of classification.

Table 3: The comparison of classification results using SVM

Method	Classification accuracy (%)	
	Training	Testing
SVM applies for the component 4 in this study	100	98.57
SVM applied for the detail d2 (Niu et al., 2008)	100	90
SVM + PCA (Widodo et al., 2009)	100	76.19
SVM + ICA (Widodo et al., 2009)	100	83.33

3. Conclusion

This paper has presented the novel intelligent fault diagnosis framework for induction motors using the transient current signal. Its implementation follows three consecutive stages. The accuracy of the RVM classifier achieves a good result where is of 100 % in training and 98.57 % in testing. Additionally, a comparative study of the performance of this framework where SVM has been used as a classifier and those of the previous studies has been carried out. The results show that the proposed framework not only eliminates the smoothing and subtracting process used in previous works but also significantly improves the classification accuracy. Therefore, it is eminently suitable to use for real fault diagnosis applications.

References

- Baudat G., Anouar F., 2000, Generalized discriminant analysis using a kernel approach, *Neural Comp.* 12, 2385-2404.
- Bonnett A.H., 1992, Cause and analysis of stator and rotor failures in three-phase squirrel-cage induction motors, *IEEE Trans. Ind. Appl.* 28, 921-937.
- D'Elia G., Delvecchio S., Dalpiaz G., 2012, On the use of Fourier-Bessel series expansion for gear diagnostics, *Proc. Int. Conf. Cond. Monitoring Mach. Non-Station. Oper.*, March 26-28, Hammamet, Tunisia, pp. 267-275.
- Douglas H., Pillay P., 2005, The impact of wavelet selection on transient motor current signature analysis, *IEEE Int. Conf. Electr. Mach. Drives*, New York, USA.
- Henry D., Zolghadri A., Monsion M., Cazaurang F., 2002, Fault diagnosis in induction machines using the generalized structured singular value, *Control Eng. Pract.* 10, 587-598.
- Niu G., Widodo A., Son J.-D., Yang B.-S., Hwang D.-H., Kang D.-S., 2008, Decision-level fusion based on wavelet decomposition for induction motor fault diagnosis using transient current signal, *Expert Syst. Appl.* 35, 918-928
- Pachori R.B., Sircar P., 2008, EEG signal analysis using FB expansion and second-order linear TVAR process, *Signal Process.* 88, 415-420.
- Rato R.T., Ortigueira M.D., Batista A.G., 2008, On the HTT, its problems, and some solutions, *Mech. Syst. Signal Process.* 22, 1374-1394.
- Schoen R.R., Habetler T.G., Kamran F., Bartheld R.G., 1995, Motor bearing damage detection using stator current monitoring, *IEEE Trans. Ind. Appl.* 36, 1274-1279.
- Thomson W.T., Fenger M., 2001, Current signature analysis to detect induction motor faults, *IEEE Trans. Ind. Appl.* 7, 26-34.
- Tipping M.E., 2001, Sparse Bayesian learning and relevance vector machine, *J. Mach. Learn. Res.* 1, 211-244.
- Widodo A., Yang B.-S., Gu D.-S., Choi B.-K., 2009, Intelligent fault diagnosis system of induction motor based on transient current signal, *Mechatron.* 19, 680-689.